

## Emission of light charged particles in photon induced fission

M. Verboven, E. Jacobs, and D. De Frenne

*Nuclear Physics Laboratory, Proeftuinstraat 86, B-9000 Gent, Belgium*

(Received 10 September 1993)

The emission of light charged particles in the photofission of  $^{230,232}\text{Th}$ ,  $^{233,234,235,238}\text{U}$ ,  $^{237}\text{Np}$ , and  $^{242}\text{Pu}$  has been studied with bremsstrahlung with end-point energy of 12, 15, and 20 MeV. The light charged particles are measured using a setup consisting of eight  $\Delta E$ - $E$  particle identification detector telescopes. The kinetic energy distributions and the emission probabilities of tritons and long-range alpha particles were determined. The presence of photoprotons obscures the identification of ternary protons while  $^6\text{He}$  particles were observed clearly, however, with insufficient statistics to allow meaningful conclusions concerning their energy distribution or emission probability. The average kinetic energy of the ternary tritons and  $\alpha$  particles and the width of the triton kinetic energy distributions seems to be practically independent of the compound nucleus excitation energy or  $Z^2/A$ . Only the width of the long-range alpha particle kinetic energy distribution shows a slight increase with increasing  $Z^2/A$  of the compound nucleus. Our results point toward a slight increase of the ternary alpha particle yield with increasing excitation energy of the compound nucleus. As already observed by Wild *et al.* for spontaneously fissioning nuclei, this yield shows a clear correlation with  $\langle Q \rangle - \langle E_{\text{tot}}^* \rangle$ , where  $E_{\text{tot}}^*$  is the total kinetic energy, suggesting that the light charged particle emission probability is determined by the deformation of the system at scission, and that, for the compound nucleus excitation energy studied in our experiments, the excitation energy transferred to the compound nucleus remains in the system as internal heat, and is not transformed into deformation energy. The triton emission to binary fission ratio,  $t/B$ , for  $^{237}\text{Np}$  is not substantially higher than for the neighboring nuclei, indicating that the unpaired proton in  $^{237}\text{Np}$  does not influence in an important way the triton emission probability.

PACS number(s): 25.85.Jg, 27.90.+b

### I. INTRODUCTION

Although in spontaneous and low energy induced fission only in one out of about 500 fission events are the two fragments accompanied by a light charged particle (LCP), predominantly a high energetic  $\alpha$  particle (LRA, long-range alpha particle), this phenomenon has been studied extensively for the spontaneous fission of  $^{252}\text{Cf}$  and for the thermal neutron induced fission of the fissile actinides like  $^{235}\text{U}$  and  $^{239}\text{Pu}$  (see, e.g., [1,2]). This was stimulated by the expectation of being able to deduce information about the scission configuration from these measurements via trajectory calculations. It was assumed that this information would also be valid in the case of binary fission, in which only the two heavy fragments and no light charged particle are emitted. Meanwhile, it became clear that trajectory calculations cannot yield unambiguous information on the scission configuration, and that light particle accompanied fission is a specific process, in which the light charged particle is not a spectator but an active participant. This process is not necessary representative for binary fission (see, e.g., [2]). Comprehensive data sets, yielding a complete kinematic description of the three-body breakup, are now available from multiparameter experiments, in which the kinetic energies and angles of the LCP and the two fragments were measured. Much less detailed information is available concerning the compound nucleus  $Z$ ,  $A$ , and excitation energy dependence of the LCP emission during the fission process.

Light charged particle emission in fission is a fast pro-

cess that takes place in the final stages of the fission reaction. The energy required to release particles turns out to be a very large fraction of the available energy. This energy therefore must be stored in readily available energy sources, involving only a few degrees of freedom. These conditions are fulfilled by the few deformational degrees of freedom of the fissioning system, and not by the complex spectrum of nuclear states reached by the excitation of quasiparticles (see, e.g., [1-6]). As a consequence, the LCP-emission probability will strongly depend on the deformation energy of the fissioning nucleus at the scission point. In this sense a correlation of the LCP yield can be expected with all kind of parameters, such as  $\langle \nu \rangle$ ,  $Z^2/A$ ,  $\dots$ , that show a more or less expressed dependence on the deformation energy of the system at the moment of scission [2,4].

Based on these ideas, Wild *et al.* [5] plotted for the spontaneous fission of a number of actinides the ternary to binary fission yield ratio ( $T/B$ ) as a function of the difference between the average reaction  $Q$  value and the average total kinetic energy of the binary fragments  $\langle Q \rangle - \langle E_{\text{tot}} \rangle$ , where  $E_{\text{tot}}$  is the total kinetic energy. The quantity  $\langle Q \rangle - \langle E_{\text{tot}} \rangle$  contains the intrinsic excitation and deformation energy, but for spontaneous fission it represents to a large extent the deformation energy at scission [7,8]. Wild *et al.* found indeed a correlation between  $T/B$  and  $\langle Q \rangle - \langle E_{\text{tot}} \rangle$ .

The compound nucleus excitation energy dependence of the LCP emission appears to be fairly weak. The LCP emission for spontaneous fission seems to be about 25%

higher than for thermal neutron induced fission. Above 15 MeV excitation energy some evidence for an increase in the LCP yields has been found [3]. It is generally assumed that the intrinsic excitation energy of a compound nucleus at the barrier remains in the nucleus during the descent from saddle to scission point as intrinsic excitation energy, and is only to a very small amount transferred into deformation energy. This means, in the picture of Wild *et al.* [5], that it can be expected that the yield of the LCP's emitted during the fission process at different excitation energies will only be influenced by the changes of  $\langle Q \rangle$  and  $\langle E_{\text{tot}} \rangle$  at different excitation energies, and not by the differences in excitation energy itself. This provides us with a convenient basis to compare at the same time LCP emission in spontaneous fission and in induced fission at different excitation energies. This will be treated in more detail in the discussion of our results.

The LCP yield is the only parameter that seems to change with  $Z$  and  $A$  of the compound nucleus. The LCP-energy distribution  $\{ \langle E \rangle, \sigma(E) \}$  seems to remain remarkably invariant over a considerable range of fissioning nuclides [1,4].

Influenced by the theoretical treatment by Cârjan [9], who described the emission of ternary  $\alpha$  particles as a process of  $\alpha$  decay of the compound nucleus in the scission region, Wagemans [10] proposed and could show a correlation between the LRA-emission probability and the ground state  $\alpha$ -decay constant  $\lambda$  of the compound nucleus.

Light charged particle emission in photon induced fission was only studied by Titterton and Howard [11] and by D'hondt *et al.* [12]. Titterton and Howard investigated the emission of LCP's for the photofission of  $^{235}\text{U}$  with 23 MeV bremsstrahlung, using photographic emulsions (they observed 4 LCP's), and D'hondt *et al.*, in this laboratory, measured the energy of the LRA particles, together with the LRA to binary fission yield ratio, for the photofission of  $^{235}\text{U}$  with 20 MeV bremsstrahlung. They used one single  $\Delta E$ - $E$  detector telescope setup to identify the ternary  $\alpha$  particles.

To study at the same time the excitation energy and compound nucleus mass and charge dependence of LCP emission, we have measured the energy distributions and the yields of LCP's emitted in the photofission of  $^{230,232}\text{Th}$ ,  $^{233,234,235,238}\text{U}$ ,  $^{237}\text{Np}$ , and  $^{242}\text{Pu}$  with 12, 15, and 20 MeV bremsstrahlung. A setup consisting of eight  $\Delta E$ - $E$  detector telescopes was used. Part of the results have been previously communicated in Refs. [13] and [14].

## II. EXPERIMENTAL SETUP AND METHODS

Experiments were performed with electrons of 12, 15, and 20 MeV energy at the linac of the Nuclear Physics Laboratory of the Gent University. The bremsstrahlung was produced in a 0.1-mm-thick gold foil, cleared of electrons using a cleaning magnet, and collimated to a diameter of 2 cm at the target position. The actinide targets were placed at  $90^\circ$  with respect to the bremsstrahlung beam, with the active layer directed towards the pho-

ton beam. They consisted of an actinide oxide, acetate, or fluoride layer with a thickness of the order of 400–500  $\mu\text{g}/\text{cm}^2$  (see Table I) on a 50  $\mu\text{g}/\text{cm}^2$  polyimide backing. Eight  $\Delta E$ - $E$  detector telescopes similar to the one described in Ref. [12], were used to identify the LCP's, and to measure their kinetic energy. They were placed axially symmetrically around the beam axis, facing the active layer of the target, at an angle of  $45^\circ$  with respect to the target surface. The fission fragments were counted using a 600  $\text{mm}^2$  heavy ion surface barrier detector, placed on the back side of the target, at an angle of  $45^\circ$  with the target surface. The  $\Delta E$  (totally depleted, transmission type) detectors had a thickness between 27.4 and 32.1  $\mu\text{m}$ . The thickness of the  $E$  detectors was typically 500  $\mu\text{m}$ . The thickness of the  $E$  detectors is sufficient to stop all LCP's that we want to study. The area of the  $\Delta E$ - $E$  telescopes was 150  $\text{mm}^2$ . In front of each telescope a 20  $\mu\text{m}$  aluminum absorber was placed. The absorbers are stopping (or reducing sufficiently the energy of) the fission fragments and the radioactive  $\alpha$  particles emitted by the actinide targets. These absorber foils are also needed to suppress the background due to secondary electrons produced by the photon beam in the thick actinide targets. These secondary electrons are contributing to the  $\gamma$ -flash signal due to pileup of photons scattered off the actinide target during the linac pulse.

The energy calibration of the  $E$  detectors was done using the  $\alpha$  particles of the radioactive decay of the  $^{235}\text{U}$  target and by a  $^{228}\text{Th}$  source, in combination with a precision pulser. As the highest energetic  $\alpha$  particles from  $^{228}\text{Th}$  ( $E_\alpha > 6$  MeV) are not completely stopped in the  $\Delta E$  detectors; these  $\Delta E$  detectors were calibrated in the same way as the  $E$  detectors but using only the lower energy  $\alpha$  particles.

The pulses from the  $E$  and  $\Delta$  detectors were amplified, coded, and stored event by event on a PDP11/10 system via a CAMAC interface. The  $\gamma$  flash is monitored continuously in all detectors, and its average value is subtracted on line from the measured LCP signals. The measured  $N(E, \Delta E)$  spectra are transformed into  $N(T/a, E_T)$  spectra. Here  $E_T = E + \Delta E$  is the measured kinetic energy of the LCP, and  $T/a = (E + \Delta E)^{1.73} - E^{1.73}$ , the identification signal of the LCP (here  $a$  is a constant, and  $T$  the thickness of the  $\Delta E$  detector) (see [15]). Our setup enables the identification of  $^4\text{He}$ ,  $^6\text{He}$ , and tritons in the presence of the important proton background in our experiments, as can be seen in Figs. 1 and 2, giving as an example the  $\Delta E$ - $E$  spectrum, and the identification spectrum for the photofission of  $^{235}\text{U}$  with 12 MeV bremsstrahlung. The energy spectrum of the different LCP's is corrected for their energy loss in the 20  $\mu\text{m}$  Al foils in front of the  $\Delta E$ - $E$  telescopes, a Gauss curve is fitted to the corrected energy spectrum, and the parameters of the energy distribution are determined. As an example we give in Fig. 3 the energy spectrum of the LRA particles emitted in the photofission of  $^{235}\text{U}$  with 20 MeV bremsstrahlung, and in Fig. 4 the energy spectrum of the tritons emitted in the photofission of  $^{234}\text{U}$  with 12 MeV bremsstrahlung. The total number of measured LCP's is obtained from the area of the fitted Gauss curve. In the case of ternary  $\alpha$  particles (LRA) a correc-

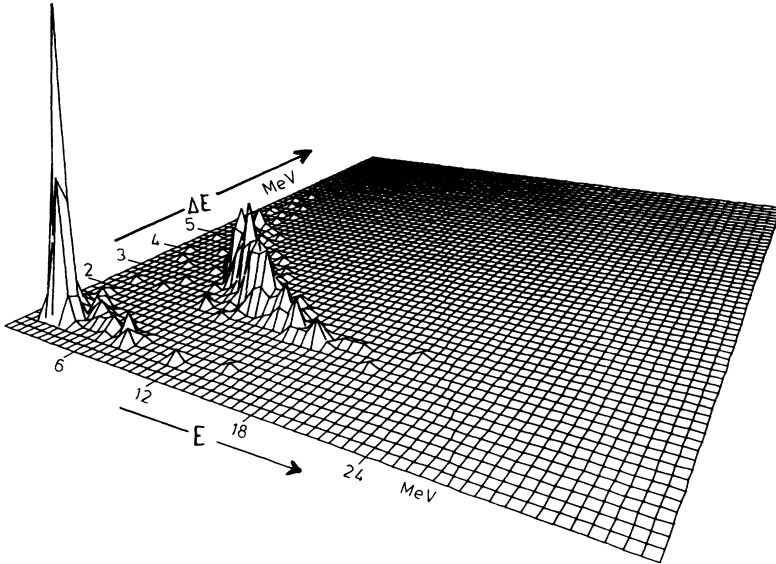


FIG. 1. Typical  $\Delta E$ - $E$  spectrum of the LCP's emitted in the photofission of  $^{235}\text{U}$  with 12 MeV bremsstrahlung.

tion of 6% was applied to this area to take into account the deviation of the energy spectrum of the LRA's from the Gaussian shape in the low energy region [16–18]. For the other LCP's no such a deviation was observed, and hence no correction was applied in our experiments. The total number of fission fragments is counted in a separate detector (see above). The LCP/B ratio (ratio of binary fission to LCP accompanied fission yield) is deduced from the count rates in the  $\Delta E$ - $E$  telescopes and in the fission fragment detector. The necessary correction factors to take into account the different geometries and the coincidence losses in the  $\Delta E$ - $E$  telescopes were determined separately.

The average excitation energy of a compound nucleus, excited with bremsstrahlung with end-point energy  $E_e$ , is given by

$$\langle E_{\text{exc}}(E_e) \rangle = \frac{\int_0^{E_e} k \sigma_{\gamma,f}(k) \Phi(E_e, k) dk}{\int_0^{E_e} \sigma_{\gamma,f}(k) \Phi(E_e, k) dk},$$

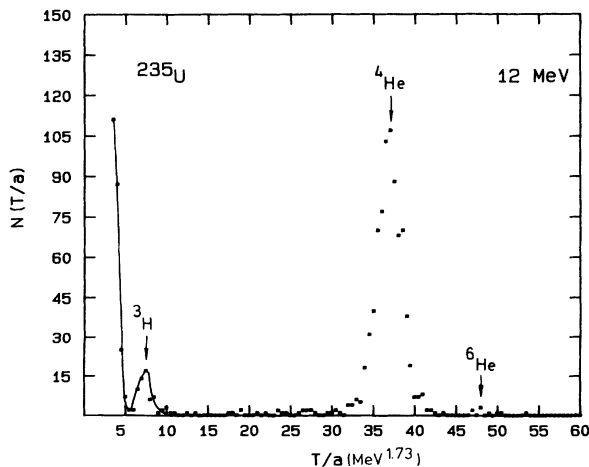


FIG. 2. Typical identification spectrum of the LCP's emitted in the photofission of  $^{235}\text{U}$  with 12 MeV bremsstrahlung.

with  $k$  the photon energy,  $\sigma_{\gamma,f}(k)$  the total photofission cross section, and  $\Phi(E_e, k)$  the bremsstrahlung spectrum. The bremsstrahlung spectrum was calculated using the EGS4 code [19]. The photofission cross sections for the different targets were taken from the work of Berman *et al.* [20], Caldwell *et al.* [21], and Thierens *et al.* [22]. For  $^{230}\text{Th}$  no  $(\gamma, f)$  cross section is known. The emission of LRA particles and tritons for the following nuclei has been studied:  $^{230,232}\text{Th}$ ,  $^{233,234,235,238}\text{U}$ ,  $^{237}\text{Np}$ , and  $^{242}\text{Pu}$ . The main characteristics of the targets and the average excitation energies of the different compound nuclei are summarized in Table I. The calculated  $\langle E_{\text{exc}}(E_e) \rangle$  values in Table I do not take into account the reduction of the average compound nucleus excitation energy due to the preceding neutron emission in the case of second chance fission.

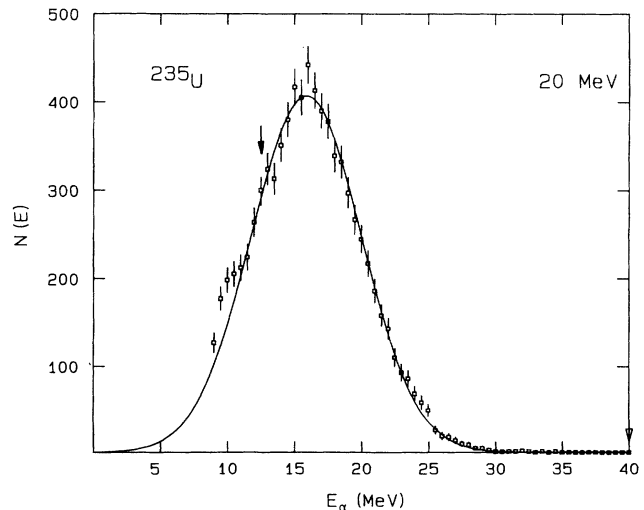


FIG. 3. The energy distribution of the LRA particles emitted in the photofission of  $^{235}\text{U}$  with 20 MeV bremsstrahlung. The line represents a Gaussian fit to the data for  $E_\alpha$  values above 12.5 MeV.

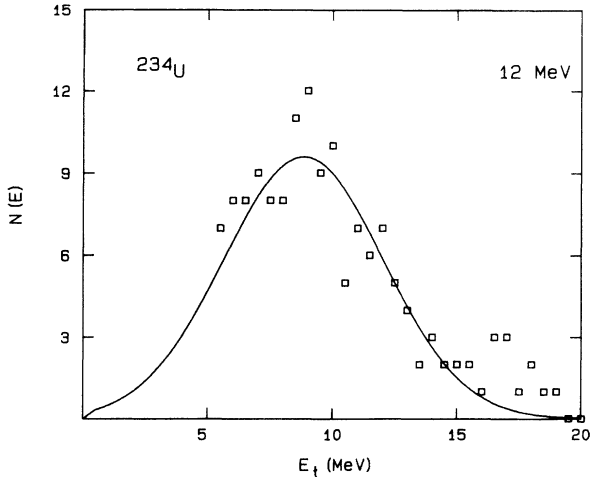


FIG. 4. The energy distribution of the tritons emitted in the photofission of  $^{234}\text{U}$  with 12 MeV bremsstrahlung. The line represents a Gaussian fit through the data for  $E_t$  values above 6.0 MeV.

A substantial contribution of second chance fission can be expected in our experiments at 15 and 20 MeV electron energy. As the  $(\gamma, nf)$  threshold lies around 12 MeV, the second chance contribution in our 12 MeV measurements can be neglected. Based on the work of Caldwell *et al.* [21], and Berman *et al.* [20], who determined neutron emission  $\Gamma_n$ , and fission widths  $\Gamma_f$ , for a number of actinides, and who deduced a relation between  $\Gamma_n/\Gamma_f$  and  $Z^2/A$ , enabling us to obtain  $\Gamma_n/\Gamma_f$  values for non-measured nuclei by interpolation, we estimated an upper limit for the second chance fission contribution in our experiments. The results are given in Table II.

The photofission cross section of the actinide nuclei studied shows a maximum value (giant  $E1$  resonance) around 14 MeV. This maximum does not exceed 400 mb. If we assume that only in one out of 500 fission events is a LCP emitted, it can be concluded that the maximum value of the cross section for LCP accompanied fission is smaller than about 1 mb. The targets used and their backings and supports contain, besides the actinide nuclei, also a number of light isotopes, such as  $^1\text{H}$ ,  $^{12}\text{C}$ ,  $^{16}\text{O}$ ,  $^{19}\text{F}$ , etc. It can be verified that the  $(\gamma, p)$  cross section on these nuclei in the energy region of our experiments

TABLE I. Characteristics of the targets and average excitation energies of the compound nuclei in our LCP emission studies.

Isotope	Enrichment (%)	Thickness ( $\mu\text{m}/\text{cm}^2$ )	$\langle E_{\text{exc}}(E_e) \rangle$ for $E_e$		
			12 MeV	15 MeV	20 MeV
$^{230}\text{Th}$	91.54	583	-	-	-
$^{232}\text{Th}$	nat.Th	413	8.8	10.7	12.4
$^{233}\text{U}$	$\sim 95\%$	453	9.5	11.3	12.6
$^{234}\text{U}$	99.07	462	9.5	11.2	12.6
$^{235}\text{U}$	97%	416	9.7	11.5	12.8
$^{238}\text{U}$	nat.U	495	9.4	11.1	12.7
$^{237}\text{Np}$	100%	382	9.4	10.9	12.3
$^{242}\text{Pu}$	99.75%	487	9.4	11.1	12.5

TABLE II. Upper limits (%) for the contribution of the second chance fission probability at different bremsstrahlung end-point energies.

Isotope	$B_F(\gamma, nf)^a$	12 MeV	15 MeV	20 MeV
$^{230}\text{Th}$	-	-	-	-
$^{232}\text{Th}$	12.6	0	14	28
$^{233}\text{U}$	11.9	1	17	21
$^{234}\text{U}$	12.5	0	21	29
$^{235}\text{U}$	11.3	12	32	36
$^{238}\text{U}$	12.3	0	27	38
$^{237}\text{Np}$	12.2	0	17	23
$^{242}\text{Pu}$	12.2	0	8	18

<sup>a</sup> $B_F(\gamma, nf)$  indicates the second chance fission barrier.

can be of the order of several mb (see, e.g., [23]). On the other hand, calculations in a preequilibrium model [24] show that at 20 MeV we can expect  $(\gamma, p)$  cross sections on the actinide nuclei of the order of 0.5 mb. All these protons have energy spectra that can overlap with the energy spectrum of the studied LCP's (especially LRA particles), showing the necessity of using  $\Delta E$ - $E$  telescopes for the detection of the ternary LCP's, proving also that we will not be able to identify ternary protons in our photofission experiments.

A contribution of the  $(\gamma, \alpha)$  process in our experiments can be excluded. This was tested using PbO targets. The  $Q(\alpha)$  values for the stable Pb isotopes are  $^{206}\text{Pb}(Q_\alpha = 1.136 \text{ MeV})$ ,  $^{207}\text{Pb}(Q_\alpha = 0.398 \text{ MeV})$ , and  $^{208}\text{Pb}(Q_\alpha = 0.519 \text{ MeV})$ . The  $Q(\alpha)$  values for the actinides studied vary between 4.082 MeV for  $^{232}\text{Th}$  and 4.983 MeV for  $^{242}\text{Pu}$  [25]. Taking into account the higher Coulomb barrier for the actinide nuclei, we may consider that the nonobservation of the  $\alpha$  particles in our test experiments using a PbO target proves that we can assume that all the observed  $\alpha$  particles in our experiments on the actinide nuclei are due to ternary fission. From calculations in the preequilibrium model a cross section  $\sigma(\gamma, \alpha) \approx 10^{-5} \text{ mb}$  is expected for  $^{232}\text{Th}$  for 25 MeV photons [24]. Thus also these calculations indicate that  $(\gamma, \alpha)$  contributions in our experiments are very unlikely.

### III. EXPERIMENTAL RESULTS AND DISCUSSION

#### A. Energy distribution of the light charged particles

##### 1. Ternary alpha particles (LRA)

In Table III the parameters of the energy distribution of the LRA particles (ternary long-range  $\alpha$  particles) observed in our experiments are summarized. For each nucleus the end-point energy  $E_e$  of the bremsstrahlung and the total number  $N_\alpha$  of LRA particles (obtained by a Gaussian extrapolation of the measured results over the whole energy region—see experimental setup and methods) are given. The average energy of the LRA particles  $\langle E_\alpha \rangle$  and the full width at half maximum (FWHM) are

TABLE III. Yields and parameters of the energy distribution of the LRA particles, observed in our photofission experiments.

Isotope	$Z^2/A$	$N_\alpha$	$E_e$ (MeV)	$\langle E_\alpha \rangle$ (MeV)	FWHM (MeV)	$10^3 \text{LRA}/B$
$^{230}\text{Th}$	35.22	902	20	$16.0 \pm 0.2$	$9.1 \pm 0.2$	$1.25 \pm 0.08$
$^{232}\text{Th}$	34.91	919	20	$16.0 \pm 0.2$	$8.9 \pm 0.3$	$1.35 \pm 0.08$
$^{233}\text{U}$	36.33	1073	12	$15.7 \pm 0.2$	$9.5 \pm 0.3$	$1.88 \pm 0.11$
$^{233}\text{U}$	36.33	2340	15	$15.5 \pm 0.2$	$9.3 \pm 0.3$	$2.07 \pm 0.07$
$^{233}\text{U}$	36.33	2774	20	$15.5 \pm 0.2$	$10.0 \pm 0.2$	$2.17 \pm 0.08$
$^{234}\text{U}$	36.17	1166	12	$15.7 \pm 0.1$	$9.4 \pm 0.3$	$1.57 \pm 0.16$
$^{234}\text{U}$	36.17	1780	15	$15.8 \pm 0.1$	$9.5 \pm 0.2$	$2.03 \pm 0.22$
$^{234}\text{U}$	36.17	2654	20	$16.0 \pm 0.1$	$9.2 \pm 0.2$	$1.62 \pm 0.19$
$^{235}\text{U}$	36.02	842	12	$15.5 \pm 0.2$	$9.5 \pm 0.2$	$1.62 \pm 0.23$
$^{235}\text{U}$	36.02	1720	15	$15.8 \pm 0.2$	$9.7 \pm 0.1$	$1.80 \pm 0.08$
$^{235}\text{U}$	36.02	8433	20	$15.9 \pm 0.1$	$9.7 \pm 0.1$	$1.86 \pm 0.24$
$^{238}\text{U}$	35.56	1531	15	$15.7 \pm 0.1$	$9.3 \pm 0.2$	$1.32 \pm 0.07$
$^{238}\text{U}$	35.56	1361	20	$16.4 \pm 0.2$	$9.2 \pm 0.2$	$1.37 \pm 0.09$
$^{237}\text{Np}$	36.49	1985	15	$16.0 \pm 0.1$	$9.6 \pm 0.2$	$1.59 \pm 0.08$
$^{237}\text{Np}$	36.49	2008	20	$15.6 \pm 0.1$	$10.2 \pm 0.2$	$1.75 \pm 0.08$
$^{242}\text{Pu}$	36.51	954	12	$15.5 \pm 0.3$	$9.7 \pm 0.2$	$1.56 \pm 0.09$
$^{242}\text{Pu}$	36.51	2109	15	$15.9 \pm 0.1$	$9.5 \pm 0.1$	$1.98 \pm 0.09$
$^{242}\text{Pu}$	36.51	1481	20	$15.9 \pm 0.1$	$10.0 \pm 0.2$	$1.91 \pm 0.08$

obtained from a Gaussian fit to the experimental data, with an energy  $E_\alpha > 12$  MeV.

The average energy of the LRA particles seems to be practically constant within the experimental accuracy. The average value of  $\langle E_\alpha \rangle$  over all our measurements is  $15.8 \pm 0.1$  MeV. For the  $^{233}\text{U}$ ,  $^{234}\text{U}$ ,  $^{235}\text{U}$ , and  $^{242}\text{Pu}$  nuclei, where measurements at the three bremsstrahlung end-point energies were performed, we calculated an average LRA energy for each bremsstrahlung end-point energy separately. The results are

$$\begin{aligned} E_e = 12 \text{ MeV}, \quad \langle E_\alpha \rangle &= 15.60 \pm 0.06 \text{ MeV}; \\ E_e = 15 \text{ MeV}, \quad \langle E_\alpha \rangle &= 15.75 \pm 0.09 \text{ MeV}; \\ E_e = 20 \text{ MeV}, \quad \langle E_\alpha \rangle &= 15.83 \pm 0.11 \text{ MeV}. \end{aligned}$$

The small differences that are observed cannot be considered to be significant; they are practically within the error bars. In addition the  $\gamma$  flash, observed in the  $E$  detectors, increases with increasing end-point energy of the bremsstrahlung, while also the  $\gamma$  flash in the  $\Delta E$  detectors starts to show up. Both contributions can be responsible for the small differences in  $\langle E_\alpha \rangle$  that can exist between the measurements at different bremsstrahlung end-point energies.

The FWHM of the LRA-particle energy distribution seems to be practically independent of the compound nucleus excitation energy. For the four nuclei for which measurements at  $E_e = 12, 15,$  and  $20$  MeV were performed, we obtain the following averaged FWHM values:

$$\begin{aligned} E_e = 12 \text{ MeV}, \quad \langle \text{FWHM} \rangle &= 9.53 \pm 0.06 \text{ MeV}; \\ E_e = 15 \text{ MeV}, \quad \langle \text{FWHM} \rangle &= 9.50 \pm 0.08 \text{ MeV}; \\ E_e = 20 \text{ MeV}, \quad \langle \text{FWHM} \rangle &= 9.73 \pm 0.19 \text{ MeV}. \end{aligned}$$

Wagemans *et al.* [18] showed that the FWHM of the LRA-particle energy distribution for  $^{233,235}\text{U}$  and  $^{239,241}\text{Pu}(n_{\text{th}}, f)$  increases with  $Z^2/A$ . They found the relation

$$\text{FWHM} = (-8 \pm 5) + (0.50 \pm 0.14) Z^2/A.$$

A least-squares fit to our experimental points leads to the following results:

$$E_e = 12 \text{ MeV},$$

$$\text{FWHM} = (-6 \pm 20) + (0.43 \pm 0.56) Z^2/A;$$

$$E_e = 15 \text{ MeV},$$

$$\text{FWHM} = (10 \pm 7) + (-0.009 \pm 0.2) Z^2/A;$$

$$E_e = 20 \text{ MeV},$$

$$\text{FWHM} = (-18 \pm 5) + (0.75 \pm 0.14) Z^2/A.$$

It turned out that only for 20 MeV bremsstrahlung could a sufficient number of nuclei be studied with high enough accuracy to observe an increase of the FWHM with  $Z^2/A$ , although here again one has to be cautious because of the broadening in the  $T/a$  particle identification spectrum, due to an increased  $\gamma$ -flash signal and the associated higher fluctuations, when working at higher bremsstrahlung end-point energy.

Trajectory calculations [26] indicate that the final energy of the LRA particle is mainly determined by its acceleration in the Coulomb field of the two fragments, the initial energy of the LRA particles being small. The observed constancy of the final LRA energy would then indicate that on the average the Coulomb field of the fission fragments in the neck region is practically constant for fissioning nuclei varying from  $^{232}\text{Th}$  to  $^{252}\text{Cf}$ . (Assuming that the majority of the LRA particles are emitted from the neck region [2].) The average position of the heavy fragment peak  $\langle M_H \rangle$  remains practically constant as a function of the compound nucleus charge and mass [27]. The assumption that the  $A/Z$  ratio of the fissioning nucleus is conserved in the fragments [28] leads to the conclusion that also the average position of the heavy fragment charge  $\langle Z_H \rangle$  will remain practically constant when going from  $^{232}\text{Th}$  to  $^{252}\text{Cf}$ , while the average mass and charge of the light fragment will increase. The constancy of the average Coulomb field between the two fragments is only possible when the scission configuration of the heavier fissioning nuclei is more elongated. The higher charge of the light fragment is then compensated by the increased distance between the fragments and the LRA particle.

The width of the final energy distribution of the LRA particles is predominantly determined by the fluctuations of the initial energies of the LRA particles. These small fluctuations are amplified by the Coulomb field. The cal-

culations of Pik-Pichak [26] show that an increase of these fluctuations can be related to an increase of the initial distance between the fragments with increasing mass of the fissioning nucleus. On the other hand, the liquid drop model expects an increase of the pre-scission kinetic energy with increasing  $Z^2/A$  (see Ref. [29]).

Extended studies of the LRA-energy distribution for  $^{235}\text{U}$  (see Refs. [16,17]),  $^{233}\text{U}$  and  $^{239}\text{Pu}(n_{\text{th}}, f)$  (see [18]) have shown that at the low energy side (below about 11 MeV) this energy distribution shows a deviation from a Gaussian shape, resulting in a 6% higher yield than expected from a Gaussian fit to the higher energy points. In Fig. 3 we show the energy spectrum of the LRA particles emitted in the photofission of  $^{235}\text{U}$  with 20 MeV bremsstrahlung. It is clear that also our results show the deviation of the LRA-energy spectrum from the Gaussian shape in the low energy part of the spectrum. As done in Refs. [30,31] we fitted several Gauss distributions to these LRA-energy data points, starting at different LRA energies. We found as in Refs. [30,31] that when decreasing the lower limit of the fitting interval, the width of the fitted Gauss curve increases, indicating an increased yield of low energy LRA particles. As we are using a shielded detector telescope, only LRA particles with an energy above 9 MeV could be observed. For this reason we did not estimate the size of the deviation of the LRA-energy distribution from the Gaussian shape.

## 2. Other light charged particles

With the detector telescopes used in our experiments we could also observe tritons. However, due to interfering ( $\gamma, p$ ) reactions this was only possible for 12 and 15 MeV bremsstrahlung, and not for 20 MeV bremsstrahlung. Even at 15 MeV there was already a partial interference of the identification signal of the tritons and the ( $\gamma, p$ ) protons. As a consequence at this bremsstrahlung end-point energy only tritons with an energy above 6 MeV could be measured. As an example the energy distribution of the tritons for the photofission of  $^{234}\text{U}$  with 12 MeV bremsstrahlung is given in Fig. 4.

In Table IV we have summarized our results concerning the parameters of the energy distribution of the tri-

tons emitted in photofission. The average triton energy  $\langle E_t \rangle$  and the full width at half maximum (FWHM) of the triton energy distribution, together with the number of tritons obtained by a Gaussian fit to the data points with an energy  $E_t > 6.0$  MeV,  $N_t$ , and the bremsstrahlung end-point energy  $E_e$ , are given. The average triton energy over all our measurements is  $8.2 \pm 0.2$  MeV, while the average of the FWHM of the triton energy distribution over all our measurements is  $5.9 \pm 0.4$  MeV. The average energy and the width of the energy distribution seem to be independent of  $E_e$  or  $Z^2/A$ ; however, the accuracy of our results is too low to allow a conclusion concerning the dependence of these parameters on the fissioning nucleus  $Z^2/A$  or excitation energy.

## B. Yield of the light charged particles

### 1. Ternary alpha particles

The last column of table III gives the number of ternary LRA particles per 1000 binary fission events  $\text{LRA}/B$ . As described in Sec. II, the number of LRA's is obtained via a Gaussian fit to the data points of the LRA-energy spectrum ( $E_{\text{LRA}} > 12.5$  MeV), and a correction of the result for the deviation of this spectrum from the Gaussian shape in the low energy region. In the  $\text{LRA}/B$  ratio also a correction for different geometry between the fission detector and the LCP detector telescopes is included.

Concerning the compound nucleus excitation energy dependence of the LRA-particle yields, not much information is available. It is known that the LRA yield for spontaneous fission is about 25% higher than for the fission of the same compound nucleus induced by thermal neutron capture (see Introduction). Based on results on the LRA emission in  $p$ - and  $\alpha$ -induced fission of  $^{232}\text{Th}$  and  $^{238}\text{U}$ , Rajagopalan and Thomas [32] came to the conclusion that for compound nucleus excitation energies  $E_{\text{exc}}$  above about 15 MeV, the LRA yield changes only slightly with  $E_{\text{exc}}$ . The changes can be represented by

$$Y_\alpha = 1.82 \pm 0.13 + (0.019 \pm 0.006)E_{\text{exc}},$$

where the yields  $Y_\alpha$  are given in  $\alpha$ 's per 1000 fission events and  $E_{\text{exc}}$  in MeV. For the  $E_{\text{exc}}$  region between about 6 MeV (thermal neutron induced fission) and about 15 MeV, no information is available concerning the  $E_{\text{exc}}$  dependence of the LRA yields.

We have fitted a straight line through our results for the different nuclei as a function of the average compound nucleus excitation energy. The slopes of these lines are given in Table V. In this fitting we did not take into account a possible second chance fission effect. Our results point towards a slight increase of the LRA yield with increasing  $\langle E_{\text{exc}} \rangle$ . The slight increase of the  $\text{LRA}/B$  ratio with  $\langle E_{\text{exc}} \rangle$  is in agreement with the assumption that the LRA yield depends on the deformation energy of the system at the scission point [5]. The decrease of the average kinetic energy of the fragments with increasing  $\langle E_{\text{exc}} \rangle$

TABLE IV. Yields and parameters of the energy distribution of the  $^3\text{H}$  particles observed in our photofission experiments.

Isotope	$Z^2/A$	$N_t$	$E_e$ (MeV)	$\langle E_t \rangle$ (MeV)	FWHM (MeV)	$10^3 t/B$
$^{233}\text{U}$	36.33	67	12	$7.8 \pm 1.0$	$5.1 \pm 1.0$	$0.12 \pm 0.02$
$^{233}\text{U}$	36.33	210	15	$8.0 \pm 1.0$	$6.0 \pm 1.0$	$0.19 \pm 0.03$
$^{234}\text{U}$	36.17	154	12	$8.8 \pm 1.0$	$7.6 \pm 1.0$	$0.21 \pm 0.04$
$^{234}\text{U}$	36.17	184	15	$8.1 \pm 1.0$	$5.1 \pm 1.0$	$0.21 \pm 0.03$
$^{235}\text{U}$	36.02	69	12	$7.7 \pm 1.0$	$7.1 \pm 1.0$	$0.13 \pm 0.03$
$^{235}\text{U}$	36.02	163	15	$7.6 \pm 1.0$	$6.4 \pm 1.0$	$0.17 \pm 0.03$
$^{238}\text{U}$	35.56	138	15	$9.4 \pm 1.0$	$5.8 \pm 1.0$	$0.12 \pm 0.02$
$^{237}\text{Np}$	36.49	176	15	$7.8 \pm 1.0$	$6.5 \pm 1.0$	$0.15 \pm 0.03$
$^{242}\text{Pu}$	36.51	86	12	$8.6 \pm 1.0$	$5.4 \pm 1.0$	$0.14 \pm 0.02$
$^{242}\text{Pu}$	36.51	171	15	$8.0 \pm 1.0$	$3.5 \pm 1.0$	$0.16 \pm 0.03$

TABLE V. Slope of the straight line fitted to the LRA/B results as a function of  $\langle E_{exc} \rangle$ .

Isotope	Slope
$^{233}\text{U}$	$0.09 \pm 0.04$
$^{234}\text{U}$	$0.03 \pm 0.08$
$^{235}\text{U}$	$0.08 \pm 0.10$
$^{238}\text{U}$	$0.03 \pm 0.07$
$^{237}\text{Np}$	$0.11 \pm 0.08$
$^{242}\text{Pu}$	$0.11 \pm 0.04$

[28] shows that indeed the deformation of the system decreases slightly with increasing  $\langle E_{exc} \rangle$ .

As discussed in the Introduction, the LRA yield can be related to all kind of parameters that are influenced by the deformation of the system at scission. Liquid drop model calculations show that the deformation energy at scission increases with increasing fissility parameter  $Z^2/A$  [29]. Our results too show an increasing LRA yield with increasing  $Z^2/A$ . However, when we take only the results for the U isotopes, the increase of the LRA yield with  $Z^2/A$  is about a factor of 2 higher. This is illustrated in Fig. 5, in which our LRA-yield results for 20 MeV bremsstrahlung induced fission are plotted as a function of  $Z^2/A$ . In this figure the solid line indicates a fit of a linear relation between LRA/B and  $Z^2/A$  to all the data, and the dashed line a fit restricted to the U data. It should be remarked here that in all our measurements the linear fit through the U data alone is much better than a fit through all the data.

Wagemans attributed the deviation of the behavior of the LRA/B ratio from the expected liquid drop behavior (and the expected correlation with  $Z^2/A$ ) to neutron shell effects [1]. He explained the increasing LRA/B ratio in the spontaneous fission of Pu isotopes, when going from the heavier to the lighter Pu-isotopes, by the de-

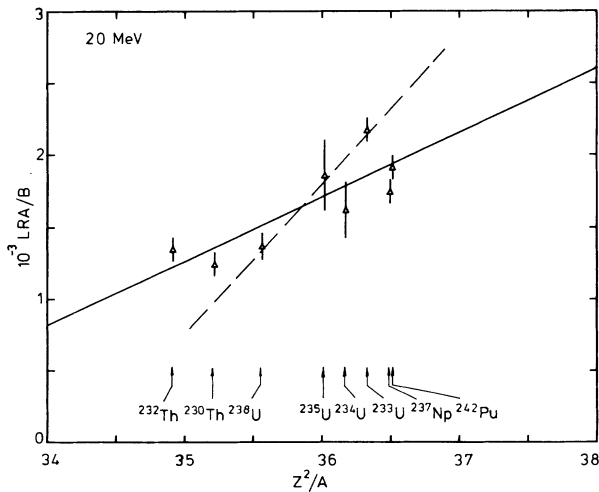


FIG. 5. LRA/B ratio as a function of  $Z^2/A$  for the photofission of  $^{230,232}\text{Th}$ ,  $^{233,234,235,238}\text{U}$ ,  $^{237}\text{Np}$ , and  $^{242}\text{Pu}$  with 20 MeV bremsstrahlung. The solid line represents a linear fit to all the data, the dashed line a fit restricted to the U data.

creasing influence of the spherical  $N=82$  shell, expressed by the decreasing yield in the mass region around 134, and by a decreasing kinetic energy of the fragments. Also for the photofission of  $^{238}\text{U}$  an increased yield of masses with  $N=82$  was observed, while this was not the case for  $^{234}\text{U}$  and  $^{235}\text{U}(\gamma, f)$  (see Refs. [33,34]). Also the average kinetic energy of the fragments is higher for  $^{238}\text{U}$ :  $\langle E_{tot} \rangle = 168.49 \pm 0.30$  MeV for  $^{234}\text{U}$ ,  $170.03 \pm 0.65$  MeV for  $^{235}\text{U}$ , and  $171.78 \pm 0.56$  MeV for  $^{238}\text{U}$ . All these values are for 12 MeV bremsstrahlung. We should remark that the value for  $^{234}\text{U}$  has to be increased with about 2 MeV when comparing with the results of  $^{235}\text{U}$  and  $^{238}\text{U}$ , because of the use of the Schmitt calibration procedure with the  $^{235}\text{U}(n_{th}, f)$  parameters for  $^{235}\text{U}$  and  $^{238}\text{U}$ , and with the  $^{252}\text{Cf}$  spontaneous fission parameters for  $^{234}\text{U}$  [35]. Here too this would indicate that in the case of the photofission of  $^{238}\text{U}$  the fragments are less deformed, resulting in a lower probability of the emission of a ternary particle.

We investigated a possible correlation between our LRA yield results and parameters of the natural  $\alpha$  decay ( $\ln \lambda$ , with  $\lambda$  the decay constant, or  $\ln P$ , with  $P$  the penetrability of the Coulomb barrier for the  $\alpha$  particle). We came to the conclusion that the correlation of our LRA/B results with  $\ln \lambda$  or  $\ln P$  is not convincing. This is not really surprising as the  $\lambda$  values used are those for the ground state  $\alpha$  decay of the actinide nucleus, while an excited actinide nucleus at the scission point has a really different configuration compared to its ground state configuration. Also the nuclear potential felt by the  $\alpha$  particle in a nucleus at the scission point is likely to be very different from the potential felt in a nucleus in the ground state.

If we assume that the LCP-emission probability is determined by the deformation energy at scission, and if we assume that  $\langle Q \rangle - \langle E_{tot} \rangle$  is a good estimate for the total deformation energy at scission for spontaneous fissioning systems, we have to expect a correlation between the LCP-emission probability and  $\langle Q \rangle - \langle E_{tot} \rangle$  (see Introduction). If we assume in addition that for the compound nucleus excitation energies in our experiments the excitation energy of the compound nucleus is transformed into internal heat [36], we come to the conclusion that also for higher energy induced fission, like in our experiments, there should be a correlation between the LCP yields and  $\langle Q \rangle - \langle E_{tot} \rangle$ .

In Table VI we summarize, for the different nuclei and bremsstrahlung end-point energies,  $E_e$ , the LCP to binary fission yield ratio LCP/B, and the  $\langle Q \rangle - \langle E_{tot}^* \rangle$  values deduced from our experiments. As usual the asterisk indicates preneutron values. As for  $^{230}\text{Th}$ ,  $^{233}\text{U}$ , and  $^{237}\text{Np}$  no photofission mass and  $E_{tot}$  data are available; these nuclei are not included in the table. The  $\langle Q \rangle$  values were calculated based on the tables of Möller and Nix [37], averaging over the mass and charge distributions. The most probable fragment  $Z$  values were calculated following the method proposed by Nethaway [38]. The mass distributions and the  $\langle E_{tot}^* \rangle$  values were obtained from the results of Refs. [6,34,39–41]. Analogous to the work of Wild *et al.* [5], the  $\langle E_{tot}^* \rangle$  values were reduced by a factor 1.0104, to correct for the difference between

TABLE VI. LCP emission probabilities and  $\langle Q \rangle - \langle E_{\text{tot}}^* \rangle$  values for the photofission of a number of actinides. For the number between parentheses in the first column, refer to Fig. 7.

Isotope	$E_e$ (MeV)	$\langle Q \rangle$ (MeV)	$\langle E_{\text{tot}}^* \rangle$ (MeV)	$\langle Q \rangle - \langle E_{\text{tot}}^* \rangle$ (MeV)	$10^3 \text{LCP}/B$
$^{232}\text{Th}(3)$	20	174.32	159.44	14.88	$1.53 \pm 0.10$
$^{234}\text{U}(6)$	12	187.59	168.62	18.97	$1.86 \pm 0.22$
$^{234}\text{U}(8)$	15	187.55	168.32	19.23	$2.34 \pm 0.28$
$^{234}\text{U}(10)$	20	187.62	168.15	19.47	$1.83 \pm 0.23$
$^{235}\text{U}(2)$	12	188.05	171.30	16.75	$1.84 \pm 0.28$
$^{235}\text{U}(5)$	15	187.90	170.97	16.93	$2.07 \pm 0.13$
$^{235}\text{U}(7)$	20	187.93	170.51	17.42	$2.10 \pm 0.29$
$^{238}\text{U}(1)$	15	186.63	172.10	14.53	$1.51 \pm 0.10$
$^{238}\text{U}(4)$	20	186.53	171.60	14.93	$1.55 \pm 0.11$
$^{242}\text{Pu}(9)$	12	197.59	175.03	22.56	$1.78 \pm 0.13$
$^{242}\text{Pu}(11)$	15	197.48	174.47	23.01	$2.24 \pm 0.14$
$^{242}\text{Pu}(12)$	20	197.46	174.09	23.37	$2.16 \pm 0.11$

the fission fragment energy calibration based on the parameters of Schmitt *et al.* [35] and the recent calibration parameters by Henschel *et al.* [42]. The inaccuracy on the  $\langle E_{\text{tot}}^* \rangle$  values is assumed to be of the order of 0.5 MeV. For calculating the LCP/B ratio the following procedure, analogous to the one used by Wild *et al.* [5], was applied: In the cases where we measured the triton yields (see further Sec. II B), the  $^3\text{H}$  yields were added to the LRA yields and the result was multiplied by a factor  $1.053 \pm 0.006$ , while in the other cases the measured LRA yields were multiplied by a factor  $1.130 \pm 0.009$ . Both procedures yielded within the experimental accuracy the same results in those cases where both LRA and  $^3\text{H}$  yields were measured.

In Fig. 6 we plotted the LCP/B ratios obtained in our measurements together with these ratios for the sponta-

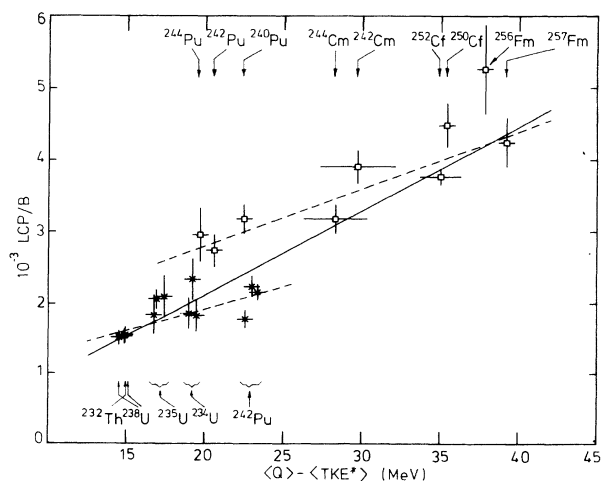


FIG. 6. LCP/B ratio as a function of  $\langle Q \rangle - \langle E_{\text{tot}}^* \rangle$  for the spontaneous fission (open squares) and the photofission (crosses) of a number of actinides. The solid line is a linear least-squares fit to all the data, the dashed line is a linear least-squares fit to the spontaneous fission and the photofission results separately.

neous fissioning systems as summarized by Wild *et al.* [5] and  $^{244}\text{Pu}$  spontaneous fission [43], as a function of  $\langle Q \rangle - \langle E_{\text{tot}}^* \rangle$ . The solid line represents a linear least-squares fit through all the data points. Although there is a considerable amount of dispersion about the linear least-squares fit, it is clear that there is a correlation between the LCP/B value and  $\langle Q \rangle - \langle E_{\text{tot}}^* \rangle$  for the whole set of data. In first order the assumption that the added excitation energy in our experiments remains in the system as internal heat and does not add to the deformation energy, although it is a drastic and crude assumption, seems to be correct. If we had plotted the LCP yield as a function of  $\langle Q \rangle - \langle E_{\text{tot}}^* \rangle + \langle E_{\text{exc}} \rangle$ , indicating that the  $E_{\text{exc}}$  would have been transformed into deformation energy, the photofission points in Fig. 6 would remain at the same height (same LCP/B value) but at a  $\langle Q \rangle - \langle E_{\text{tot}}^* \rangle$  value about 10 MeV higher, as can be seen in Fig. 7. In this figure we plotted the LCP/B results of Fig. 6 as a function of  $\langle Q \rangle - \langle E_{\text{tot}}^* \rangle + \langle E_{\text{exc}} \rangle$ . Here the relation between the LCP yield and  $\langle Q \rangle - \langle E_{\text{tot}}^* \rangle + \langle E_{\text{exc}} \rangle$  is clearly different for spontaneous fission and for induced fission. We determined also the LCP/B ratios and  $\langle Q \rangle - \langle E_{\text{tot}}^* \rangle$  for a number of thermal neutron induced fission reactions, studied by Wagemans *et al.* [18,44]. To avoid an overloaded figure we did not include the results in Fig. 6 or 7, but the results follow the tendency outlined in the foregoing discussion.

We have to stress here that the assumption that  $\langle Q \rangle - \langle E_{\text{tot}}^* \rangle$  represents the total deformation energy, or a constant important fraction of it, for all the studied fissioning systems [spontaneous fission,  $(n_{\text{th}}, f)$ , and photofission], together with the assumption that the excitation energy of the compound nucleus remains in the system as intrinsic excitation energy, and is not transformed into deformation energy, are very crude assump-

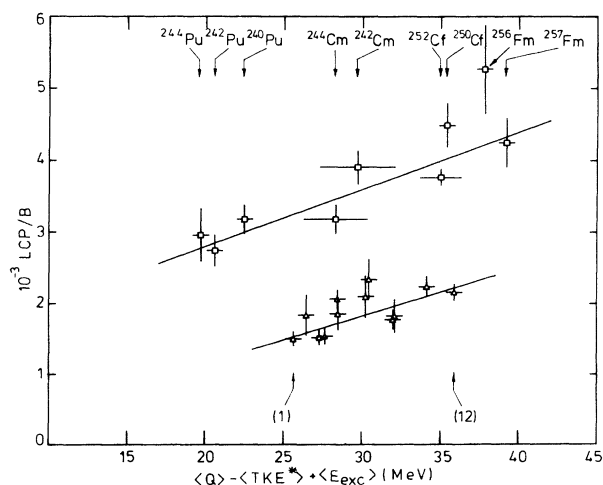


FIG. 7. LCP/B ratio as a function of  $\langle Q \rangle - \langle E_{\text{tot}}^* \rangle + \langle E_{\text{exc}} \rangle$  for the spontaneous (open squares) and the photon induced fission (open triangles) of a number of actinides. The lines represent linear least-squares fits to the spontaneous and photofission data. The numbers between brackets refer to Table VI.



tions. They seem, however, to a first approximation to provide the possibility to observe a correlation between the LCP yields of different fissioning systems. When looking closer to the results there remain smaller, but still significant, deviations between induced and spontaneous fission. In Fig. 6 the solid line indicates the linear least-squares fit to all the data, while the dashed lines represent the linear least-squares fits through the spontaneous fission and photofission results separately. It is clear that, although the fit to all the data is reasonable, the deviations between the two fits represented by the dashed lines are significant within the experimental accuracy of the data. Also the linear least-squares fit to the thermal neutron fission data deviates from both mentioned fits: It lies between the fit to the spontaneous fission data and the fit for our photofission data, closer to the later fit.

## 2. Yield of other light charged particles

In addition to LRA particles we observed in our photofission experiments also  $^3\text{H}$  and  $^6\text{He}$  particles. We will restrict ourselves here to the tritons, as the statistical accuracy for the  $^6\text{He}$  particles is too low to permit any meaningful conclusion. In Table IV we include our results concerning the yield of ternary tritons, emitted in the photofission of a number of actinide nuclei. As discussed in Sec. III A 2 only the results for 12 and 15 MeV end-point bremsstrahlung can be considered. In the last column of Table IV the triton yield per 1000 fission events  $t/B$  is given.

The value for  $^{237}\text{Np}$  is interesting. As this nucleus has an unpaired proton, one could expect that, as a consequence,  $^{237}\text{Np}$  could have a considerable higher probability for the emission of a ternary triton. This is obviously not the case.

On the average the triton yield obtained in our experiments is rather high, compared to the results given by Wagemans and Mutterer and Theobald in their review papers [1,4]. We find, averaged over all our measurements, for the ratio of triton to LRA yields the value  $t/\text{LRA} = 8.8 \pm 1.3$ .

The statistical accuracy of our measurements does not

allow more detailed conclusions concerning the changes of the triton yields with the compound nucleus excitation energy or with varying  $Z$  or  $N$  of the fissioning nucleus.

## IV. CONCLUSIONS

We have performed a systematic study of the emission of LCP's (LRA, tritons) in the photofission of a series of actinide nuclei with bremsstrahlung with end-point energies of 12, 15, and 20 MeV. For  $^{230,232}\text{Th}$ ,  $^{233,234,235,238}\text{U}$ ,  $^{237}\text{Np}$ , and  $^{242}\text{Pu}(\gamma, f)$  the yield and the parameters of the energy distribution of LRA particles and tritons [ $\langle E \rangle$  and  $\sigma(E)$ ] were determined. The average LRA energy remains practically constant for all studied systems; the width of the LRA-energy distribution seems to increase slightly with increasing fissility of the fissioning nucleus. The yield of the LRA particles and LCP's shows also a slight increase with increasing compound nucleus excitation energy. This is consistent with the few results given in the literature, and it shows that for the excitation energy region of our experiments (above the barrier plus pairing gap) the increasing compound nucleus excitation energy has only a minor influence on the LRA- and LCP yield. The LRA- and LCP-emission probabilities are not very strongly correlated with one of the classically proposed parameters ( $Z^2/A$ ,  $4Z - A$ ,  $\ln \lambda$ , etc.). The only rather unambiguous conclusion at this moment is that the LCP-emission probability is correlated to the amount of deformation energy at the scission point.

## ACKNOWLEDGMENTS

Thanks are expressed to Ir. W. Mondelaers and the linac crew for the reliable operation of the accelerator, to Dr. P. D'hondt for his contribution in the first stage of this work, and to Dr. C. Wagemans for the many stimulating and fruitful discussions. This work is part of the research program of the Inter-University Institute for Nuclear Sciences-National Fund for Scientific Research. Two of us (E.J. and D.D.F.) would like to acknowledge the financial support of the National Fund for Scientific Research.

- 
- [1] C. Wagemans, in *The Nuclear Fission Process*, edited by C. Wagemans (CRC Press, Boca Raton, FL, 1991), Chap. 12, p. 580.
  - [2] J.P. Theobald, P. Heeg, and M. Mutterer, *Nucl. Phys.* **A502**, 343c (1989).
  - [3] R. Vandenbosch and J. Huizenga, *Nuclear Fission* (Academic Press, New York, 1973), Chap. XIV, p. 374.
  - [4] M. Mutterer and J. Theobald, in *Handbook of Nuclear Decay Modes*, edited by D.N. Poenaru and W. Greiner (CRC Press, Boca Raton, FL, in press).
  - [5] J.F. Wild, P.A. Baisden, R.J. Dougan, E.K. Hulet, R.W. Lougheed and J.H. Landrum, *Phys. Rev. C* **32**, 488 (1985).
  - [6] M. Piessens, E. Jacobs, S. Pommé, and D. De Frenne, *Nucl. Phys.* **A556**, 88 (1993).
  - [7] F. Gönnewein, J.P. Bocquet, and R. Brissot, in *Proceedings of the XVIIth International Symposium on Nuclear Physics*, Gaussig, 1987, edited by D. Seeliger and H. Kalka (Zentralinstitut für Kernforschung Rossendorf, Dresden, 1988), p. 129.
  - [8] H. Schultheis and R. Schultheis, *Phys. Rev. C* **18**, 1317 (1978).
  - [9] N. Cârjan, Ph.D. thesis, Technische Hochschule Darmstadt, 1977.
  - [10] C. Wagemans, in *Particle Emission from Nuclei*, edited by D. Poenaru and M. Ivascu (CRC Press, Boca Raton, FL, 1988), Vol. III, Chap. 3.
  - [11] E.W. Titterton and F.K. Howard, *Phys. Rev.* **76**, 142 (1949).
  - [12] P. D'hondt, E. Jacobs, A. De Clercq, D. De Frenne, H. Thierens, P. De Gelder, and A.J. Deruytter, *Phys. Rev. C* **21**, 963 (1980).

- [13] M. Verboven, E. Jacobs, P. D'hondt, A. De Clercq, D. De Frenne, M. Piessens, and G. De Smet, in *Proceedings of the XVth International Symposium on Nuclear Physics*, Gaussig, 1985, edited by D. Seeliger, K. Seidel, and H. Mårten (Zentralinstitut für Kernforschung-Rossendorf, Dresden, 1986), p. 96.
- [14] M. Verboven, E. Jacobs, P. D'hondt, A. De Clercq, D. De Frenne, M. Piessens, and G. De Smet, in *Proceedings of the Seminar on Fission*, Pont d'Oye (Habye-la-Neuve), 1986, edited by C. Wagemans (SCK/CEN,Mol), p. 85.
- [15] F.S. Goulding, D.A. Landis, J. Cerny, and R.H. Pehl, *Nucl. Instrum.* **31**, 1 (1964).
- [16] P. D'hondt, A. De Clercq, A. Deruytter, C. Wagemans, M. Asghar, and A. Emsallem, *Nucl. Phys.* **A303**, 275 (1978).
- [17] F. Caitucoli, B. Leroux, G. Barreau, N. Cârjan, T. Benfoughal, T. Doan, F. El Hage, A. Sicre, M. Asghar, P. Perrin, and S. Siegert, *Z. Phys. A* **298**, 219 (1980).
- [18] C. Wagemans, P. D'hondt, and P. Schillebeeckx, *Phys. Rev. C* **33**, 943 (1986).
- [19] W.R. Nelson, H. Hirayama, and D.W.O. Rogers, Report No. SLAC-Report-265, 1985.
- [20] B.L. Berman, J.T. Caldwell, E.J. Dowdy, S.S. Dietrich, P. Meyer, and R.A. Alvarez, *Phys. Rev. C* **34**, 2201 (1986).
- [21] J.T. Caldwell, E.J. Dowdy, B.L. Berman, R.A. Alvarez, and P. Meyer, *Phys. Rev. C* **21**, 1215 (1980).
- [22] H. Thierens, E. Jacobs, P. D'hondt, A. De Clercq, M. Piessens, and D. De Frenne, *Phys. Rev. C* **29**, 498 (1984).
- [23] E. Kerkhove, R. Van De Vyver, H. Ferdinande, D. Ryckbosch, P. Van Otten, P. Berkvens, and E. Van Camp, *Phys. Rev. C* **32**, 368 (1985).
- [24] D. Ryckbosch (private communication).
- [25] A.H. Wapstra and G. Audi, *Nucl. Phys.* **A432**, 1 (1985).
- [26] G.A. Pikhach, *Yad. Fiz.* **40**, 336 (1984) [*Sov. J. Nucl. Phys.* **40**, 215 (1984)].
- [27] J.P. Unik, J.E. Gindler, L.E. Glendenin, K.F. Flynn, A. Gorski, and R.K. Sjoblom, in *Proceedings of the Conference on the Physics and Chemistry of Fission*, Rochester, NY, 1973 (IAEA, Vienna 1974), Vol. II, p. 19.
- [28] F. Gönnenwein, in *The Nuclear Fission Process*, edited by C. Wagemans (CRC Press, Boca Raton, FL, 1991), Chap. 8, p. 287.
- [29] J.R. Nix, *Nucl. Phys.* **A130**, 241 (1969).
- [30] P. D'hondt, Ph.D. thesis, University Gent, 1981.
- [31] C. Chwaszczewka, M. Dakowski, T. Krogulski, E. Piasecki, M. Sowinski, A. Stegner, and J. Tys, *Acta Phys. Pol.* **25**, 187 (1969).
- [32] M. Rajagopalan and T.D. Thomas, *Phys. Rev. C* **5**, 1402 (1972).
- [33] E. Jacobs, H. Thierens, D. De Frenne, A. De Clercq, P. D'hondt, P. De Gelder, and A.J. Deruytter, *Phys. Rev. C* **21**, 237 (1980).
- [34] M. Verboven, E. Jacobs, M. Piessens, S. Pommé, and A. De Clercq, *Phys. Rev. C* **42**, 453 (1990).
- [35] H.W. Schmitt, W.M. Gibson, J.H. Neiler, F.J. Walter, and T.D. Thomas, in *Proceedings of the First Symposium on Physics and Chemistry of Fission*, Salzburg, 1965 (IAEA, Vienna, 1965), Vol. I, p. 531; H.W. Schmitt, W.E. Kicker, and C.E. Williams, *Phys. Rev.* **137**, B837 (1965).
- [36] S. Pommé, E. Jacobs, K. Persyn, D. De Frenne, K. Govaert, and M.-L. Yoneama, *Nucl. Phys.* **A 560**, 689 (1993).
- [37] P. Möller and J.R. Nix, *At. Data Nucl. Data Tables* **26**, 165 (1981).
- [38] D.R. Nethaway, University of California Radiation Laboratory Report No. UCRL-51538, 1974.
- [39] E. Jacobs, A. De Clercq, H. Thierens, D. De Frenne, P. D'hondt, P. De Gelder, and A.J. Deruytter, *Phys. Rev. C* **20**, 2249 (1979).
- [40] E. Jacobs, A. De Clercq, H. Thierens, D. De Frenne, P. D'hondt, P. De Gelder, and A.J. Deruytter, *Phys. Rev. C* **24**, 1795 (1981).
- [41] H. Thierens, E. Jacobs, P. D'hondt, A. De Clercq, M. Piessens, and D. De Frenne, *Phys. Rev. C* **29**, 498 (1984).
- [42] H. Henschel, A. Kohnle, H. Hipp, and G. Gönnenwein, *Nucl. Instrum. Methods* **190**, 125 (1981).
- [43] M. Verboven, B. Thierens, P. D'hondt, E. Jacobs, and D. De Frenne, in *Proceedings of the International Nuclear Physics Conference*, Harrogate, 1986 (contributed papers), Vol. 1, p. 431.
- [44] C. Wagemans, E. Allaert, F. Catucoli, P. D'hondt, G. Barreau, and P. Perrin, *Nucl. Phys.* **A369**, 1 (1981).